Synthesis and characterization of two ruthenium(II) heteroleptic complexes of annelated derivatives of 2,2′-bipyridine

Edmond Amouyal,*[a] Florence Penaud-Berruyer,[a] Driss Azhari,[a] Hassan Aït-Haddou,†[b] Christophe Fontenas,[b] Elena Bejan,[b] Jean-Claude Daran[b] and Gilbert G. A. Balavoine[b]

[a] *Laboratoire de Physico-Chimie des Rayonnements* (*CNRS URA 75*), *Université Paris-Sud*, *Bât. 350*, *91405 Orsay*, *France*
[b] *Laboratoire de Chimie de Coordination* (*CNRS UPR 8241*), *205 Route de Narbonne*, *31077 Toulouse cédex*, *France*

The synthesis and characterization of two annelated 2,2′-bipyridine molecules (**L**) and of the corresponding ruthenium(II) heteroleptic complexes, $[Ru(bpy)_2(\mathbf{L})][PF_6]_2$ are described. The ligands **L** bear a terbutoxypropyl chain substituent at position 2. We discovered that under basic conditions condensation between an enolisable ketone and an α,β-unsaturated ketone gives exclusively the 1,2-addition isomers with good yields. In contrast to 2,2′-bipyridine, the annelated ligands **L** show fluorescence emission, probably due to the rigidity of the molecules. Spectroscopic and photophysical results of the heteroleptic complexes at room temperature and at 77 K are similar to the reference complex, $[Ru(bpy)_3]^{2+}$, except for less intense emission quantum yields and lifetimes at room temperature. This behaviour is due to the presence of a substituent and its position adjacent to the nitrogen of the annelated ligands engaged in the coordination, rather than to the rigidity of these ligands. As shown by the crystallographic data, this substituent induces a lengthening of the adjacent Ru—N bond (2.16 Å as compared to 2.05 Å for the other Ru—N bonds). As a result, the octahedral structure of the heteroleptic complexes is distorted and the probability of nonradiative processes is thus favoured.

Synthèse et caractérisation de deux complexes hétéroleptiques de ruthénium(II) de dérivés annelés de la 2,2′-bipyridine. Nous présentons ici la synthèse et la caractérisation de deux nouveaux ligands annelés (**L**) dérivés de la 2,2'-bipyridine, ainsi que de deux complexes hétéroleptiques de ruthénium(II) correspondants, $[Ru(bpy)_2(\mathbf{L})][PF_6]_2$. Les ligands **L** comportent comme substituant en position 2 une chaîne terbutoxypropyle. Nous avons découvert que la condensation en milieu basique entre une cétone énolisable et une cétone α,β insaturée donne exclusivement les isomères de l'addition 1,2 avec de bons rendements. Contrairement à la 2,2′-bipyridine, les ligands annelés étudiés ici présentent une émission de fluorescence probablement due à la rigidité des molécules. Les résultats spectroscopiques et photophysiques des complexes hétéroleptiques à température ambiante et à 77 K sont similaires à ceux du complexe de référence, $[Ru(bpy)_3]^{2+}$, avec toutefois un rendement quantique et une durée de vie de luminescence beaucoup plus faibles que ce dernier à température ambiante. Ce comportement est plus dû à l'existence d'un substituant et à sa position adjacente à un azote des ligands annelés engagés dans la coordination, qu'à la rigidité de ces ligands. Comme le montrent les données cristallographiques, ce substituant provoque l'allongement de la liaison Ru—N adjacente (2,16 Å contre 2,05 Å pour les autres liaisons Ru—N). De ce fait, la structure octaédrique des complexes hétéroleptiques est distordue, ce qui favorise les processus de désactivation non-radiatifs.

There is a considerable interest in the synthesis and photophysics of new transition metal complexes in view of their potential utilization as photosensitizers in the design of solar energy conversion systems[1] and as components of molecular electronic devices.[2] One of the most useful ligands available to coordination chemists is 2,2′-bipyridine (bpy). Over the past two decades there has been a significant effort to develop analogues to bpy wherein differences in electronic and steric properties would lead to modification of the metal complex chemistry.[3] A large number of syntheses of annelated bis- and polypyridines[4] have been described in the literature. At the same time, few ruthenium(II) complexes prepared from these ligands have been studied.[5] In the framework of designing new constrained and heterogeneous systems, in particular for the photochemical conversion of solar energy,[1] we have synthesized new water-soluble ruthenium(II) polypyridine complexes. In these heteroleptic complexes, one of the ligands is annelated to permit a better control of its geometry. In addition, it bears a terbutoxypropyl group, which increases the solubility of the complex in water and facilitates its binding to an inorganic support. A simple synthetic approach for the construction of a central 4-aryl substituted pyridine unit was described by Thummel.[4b] A double condensation of the enamine of 6,7-dihydro-5*H*-quinolinone **1** with an aromatic aldehyde gives the 1,5-diketone precursor in the first step; then the diketone is condensed with ammonium acetate to give the desired polypyridine in reasonable yield. Ternary iminium perchlorates have been used by Risch and coworkers[6] as synthetic equivalents for aliphatic and aromatic aldehydes in a one-pot reaction, providing access to terpyridines with peripheral substituents. This procedure gives 1,4-addition and 1,2-addition isomers. The distribution of the isomeric products seems to be influenced by the nature of the

* E-mail: edmond.amouyal@lpcr.u-psud.fr
† E-mail: aithad@lcctoul.lcc-toulouse.fr

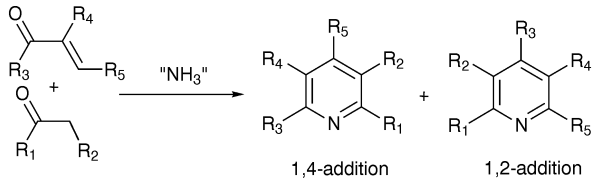

Scheme 1

substituent in the starting iminium compound. The Ru^{II} complexes with 1,2-addition isomers have been prepared and spectroscopically characterized by ^1H NMR, IR and mass spectrometry and cyclic voltammetry.[6c]

To prepare new annelated polypyridines, we explored the condensation of enolisable ketones with α,β-unsaturated ketones[7] (Scheme 1) in the presence of a nitrogen donor to obtain a highly soluble annelated polypyridine through a formal 1,4-addition reaction. We discovered that under basic conditions this condensation gives exclusively the 1,2-addition isomers with good yields. In this paper, we describe the synthesis of two annelated bipyridines, **4** and **5** (Scheme 2), and their heteroleptic complexes with ruthenium(II) of the type $[Ru(bpy)_2(\mathbf{L})][PF_6]_2$. The spectroscopic, electrochemical and photophysical properties of these ligands and complexes have also been investigated in order to examine the consequences of rigid annelated ligands on the properties of the corresponding heteroleptic complexes. We have chosen $[Ru(bpy)_3]^{2+}$ as a reference.

Experimental

Synthesis

Ligand 4. Ketone **1** (0.41 g, 13.5 mmol) and 3.05 g (13.5 mmol) of the α,β-unsaturated ketone **2** in distilled pyridine (100 mL) were heated at 90 °C in the presence of 5 equiv. of ammonium acetate for 8 h. The mixture was cooled to room temperature and the volatile components were evaporated under reduced pressure. The resulting residue was dissolved in 100 mL of dichloromethane and washed with water (2 × 50 mL). The organic phase was then dried with $MgSO_4$ and the solvent was removed under vacuum. The resulting dark oil was purified by column chromatography on deactivated Al_2O_3 using 1:1 ethyl acetate:pentane as the eluant. Yield: 65%. ^1H NMR, $CDCl_3$, δ: 8.7 (1H, d), 7.4 (1H, d), 7.17 (1H, dd), 3.46 (2H, t), 2.95 (4H, m), 2.87 (2H, m), 2.8 (2H, m), 2.68 (2H, t), 1.95 (2H, m), 1.81 (2H, t), 1.18 (9H, s). ^{13}C NMR, $CDCl_3$, δ: 158.5, 152.5, 148.5, 147.2, 143.0, 134.9, 132.5, 129.7, 122.2, 72.2, 61.2, 60.1, 32.1, 29.9, 27.4, 27.1, 26.4, 25.9, 22.4, 22.1. CI-MS: $m/z = 351$ (MH^+) Anal. Calcd for $C_{23}H_{30}N_2O$: C, 78.82; H, 8.63; N, 7.99; O, 4.56. Found: C, 78.68; H, 8.55; N, 7.72; O, 4.44.

Ligand 5. Ligand **5** was obtained by the condensation of ketone **1** with the α,β-unsaturated ketone **3** in the same manner as ligand **4**. The desired product was purified by column chromatography on Al_2O_3 using 3:1 ethyl acetate:pentane as the eluant. Yield: 70%. ^1H NMR, $CDCl_3$, δ: 8.74 (1H, d), 8.59 (1H, d), 7.62 (1H, dd), 7.57 (1H, dd), 7.21 (2H, m), 3.58 (2H, t), 3.5 (2H, t), 3.14 (2H, m), 2.92 (6H, m), 2.02 (2H, m), 1.21 (9H, s). ^{13}C NMR, $CDCl_3$, δ: 157.5, 152.7, 150.6, 148.7, 146.9, 139.8, 135.0, 134.9, 133.8, 132.1, 129.9, 122.8, 122.7, 72.5, 61.3, 33.1, 30.5, 28.4, 27.9, 27.6, 25.8, 24.3. CI-MS: $m/z = 400$ (MH^+) Anal. Calcd for $C_{26}H_{29}N_3O$: C, 78.16; H, 7.32; N, 10.52; O, 4.00. Found: C, 78.15; H, 7.27; N, 10.35; O, 4.23.

$[Ru(bpy)_2(4)][PF_6]_2$. *cis*-$(bpy)_2RuCl_2 \cdot 2H_2O$ (0.63 g, 1.2 mmol) was suspended in absolute ethanol (100 mL) and heated under argon for 30 min. Ligand **4** (0.6 g 1.44 mmol, 1.2 equiv.) was then added to the solution and the mixture was refluxed for another 16 h. The resulting solution was cooled to room temperature. After filtration, a saturated solution of ammonium hexafluorophosphate was added dropwise to the filtrate to complete precipitation. The formed precipitate was collected by filtration and dried. TLC (alumina, acetone:water:saturated aqueous potassium nitrate, 90:10:1) showed the material to be pure. Yield: 85%. ^1H NMR, CD_3CN, δ: 8.5 (4H, m), 8.05 (5H, m), 7.8 (3H, m), 7.47 (3H, m), 7.3 (3H, m), 7.15 (1H, dd), 3.18 (4H, m), 2.88 (2H, t), 2.7 (2H, m), 2.47 (2H, t,), 2.39 (2H, dd), 1.83 (4H, m), 1.2 (1H, m), 0.95 (9H, s), 0.58 (1H, m). ^{13}C NMR, CD_3CN, δ: 164.8, 158.0, 157.8, 157.7, 157.4, 156.5, 153.5, 152.2, 151.9, 151.6, 149.9, 149.3, 148.3, 138.4, 138.2, 138.0, 137.8, 137.3, 137.0, 136.6, 135.0, 128.4, 128.0, 127.9, 127.7, 126.4, 125.0, 124.8, 124.7, 72.6, 60.1, 32.4, 30.0, 27.2, 25.9, 25.8, 23.3, 22.7, 22.0. FAB-MS (NBA): $m/z = 909$ (100%, MPF_6^+), 764 (47%, $M - 2PF_6^+$)

$[Ru(bpy)_2(5)][PF_6]_2$. This complex was obtained using the same method as for $[Ru(bpy)_2(\mathbf{4})]^{2+}$. Yield: 88%. ^1H NMR, CD_3CN, δ: 8.69 (1H, dd), 8.53 (5H, m), 8.13 (3H, m), 8.06 (2H, t), 8.02 (2H, t), 7.84 (4H, m), 7.51 (3H, m), 7.43 (1H, dd), 7.35 (3H, m), 7.23 (1H, dd), 3.83 (2H, tt), 3.17 (2H, m), 2.87 (2H, m), 2.85 (2H, m), 2.63 (2H, m), 2.57 (2H, t), 1.3 (1H, m), 1.17 (9H, s), 0.59 (1H, m). ^{13}C NMR, CD_3CN, δ: 149.0, 158.0, 145.0, 144.9, 157.4, 144.8, 144.7, 144.0, 142.2, 141.0, 140.8, 140.4, 139.2, 138.2, 134.5, 131.9, 131.7, 131.6, 131.5, 130.8, 130.5, 130.1, 128.6, 125.0, 124.8, 124.6, 123.9, 122.7, 122.6, 122.5, 87.3, 78.8, 60.8, 58.5, 56.8, 56.6, 56.3, 55.6, 55.3. FAB-MS (NBA): $m/z = 958$ (100%, MPF_6^+), 813 (61%, $M - 2PF_6^+$)

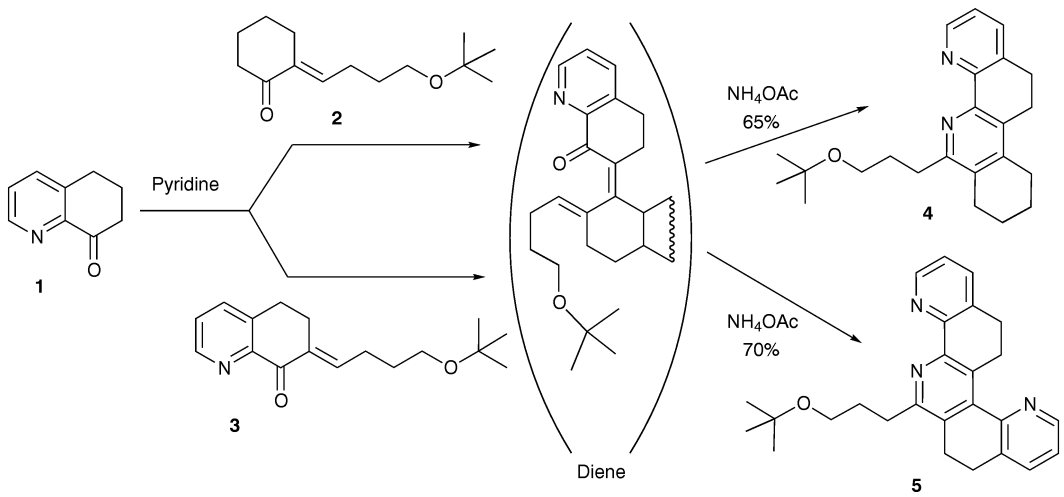

Scheme 2

X-Ray crystallography

For $[Ru(bpy)_2(\mathbf{4})]^{2+}$, data were collected at room temperature on an Enraf-Nonius CAD4 diffractometer equipped with an oriented graphite monochromator utilizing MoKα radiation (λ = 0.71073 Å). The final unit cell parameters were obtained by the least-squares refinement of the setting angles of 25 reflections that had been accurately centred on the diffractometer. Only statistical fluctuations were observed in the intensity monitors during the course of the data collection. For $[Ru(bpy)_2(\mathbf{5})]^{2+}$, data were collected at room temperature on a Stoe IPDS (imaging plate diffraction system) diffractometer equipped with an oriented graphite monochromator utilizing MoKα radiation (λ = 0.71073 Å). The final unit cell parameters were derived from the least-squares refinement of 2000 selected reflections.

The two structures were solved by direct methods (SIR92)[8] and refined by least-squares procedures on F_o. H atoms were introduced in the calculation in idealized positions [d(CH) = 0.96 Å] and their atomic coordinates were recalculated after each cycle. They were given isotropic thermal parameters 20% higher than those of the carbon to which they are attached. In $[Ru(bpy)_2(\mathbf{4})]^{2+}$, the ethanol solvent molecule presents a disordered distribution of the O atom on two sites roughly symmetrical with respect to the C—C bond of the ethyl group. In $[Ru(bpy)_2(\mathbf{5})]^{2+}$, the 2-terbutoxypropyl chain is partially disordered with the C(42), C(43), C(45), C(46) and C(47) atoms distributed on two sites related through a pseudo mirror plane containing C(38), C(41), O(1) and C(46). In both cases, it was assumed in a first step that the thermal parameters of the corresponding oxygen or carbon atoms in the disordered positions were equal and the occupancies were allowed to vary with the constraint that the sum of the occupancies equals unity. Additional distance and angle restraints (mean C—O, C—C and C—O—C or C—C—C values) were used during this procedure. When the occupancy factors were well defined, they were fixed to the observed values and the disordered atoms were allowed to refine isotropically for the ethanol solvent molecule ($[Ru(bpy)_2(\mathbf{4})]^{2+}$) and anisotropically for the 2-terbutoxypropyl chain ($[Ru(bpy)_2(\mathbf{5})]^{2+}$). No hydrogen placing was done for the C atoms of these disordered groups. Least-squares refinements were carried out by minimizing the function $\Sigma w(|F_o| - |F_c|)^2$, where F_o and F_c are the observed and calculated structure factors. The weighting scheme used in the last refinement cycles was $w = w'[1 - (\Delta F/6\sigma(F_o)^2]^2$, where $w' = 1/\Sigma_1^n A_r T_r(x)$ with three A_r coefficients for the Chebyshev polynomial $A_r T_r(x)$ and x is $F_c/F_c(\max)$.[9] Models reached convergence with $R = \Sigma(||F_o| - |F_c||)/|F_o|)$ and $R_w = \Sigma w(|F_o| - |F_c|)^2 \Sigma w(F_o)^2]^{1/2}$ having the values listed in Table 1. The criteria for a satisfactory complete analysis were ratios of rms shift to standard deviation less than 0.1 and no significant features in the final difference maps. Details of data collection and refinement are given in Table 1.

The calculations were carried out with the CRYSTALS program package[10] running on a PC. The molecules were drawn with CAMERON.[10b]

CCDC reference number 440/019.

Spectroscopy and photophysics

Electronic absoption spectra were recorded on a Perkin Elmer Lambda 9 spectrophotometer. The molar extinction coefficients ε were estimated using a concentration of 5×10^{-5} mol l^{-1} in ethanol for the ligands and a concentration of 9×10^{-5} mol l^{-1} and 8×10^{-5} mol l^{-1} in aqueous solutions for $[Ru(bpy)_2(\mathbf{4})]^{2+}$ and $[Ru(bpy)_2(\mathbf{5})]^{2+}$ complexes, respectively. In nonbuffered solutions, **5** and $[Ru(bpy)_2(\mathbf{5})]^{2+}$ are not protonated. The emission spectra, corrected from the lamp spectrum, were obtained on Jobin Yvon JY9CI or Jobin Yvon

Table 1 Crystal data for the compounds $[Ru(bpy)_2(\mathbf{4})][PF_6]_2 \cdot C_2H_5OH$ and $[Ru(bpy)_2(\mathbf{5})][PF_6]_2 \cdot (CH_3)_2CO$

Compound	$[Ru(bpy)_2(\mathbf{4})][PF_6]_2 \cdot C_2H_5OH$	$[Ru(bpy)_2(\mathbf{5})][PF_6]_2 \cdot (CH_3)_2CO$
M/g	1099.9	1161
Shape (color)	box (orange)	plate (orange)
Size/mm	0.54 × 0.42 × 0.24	0.48 × 0.36 × 0.10
Crystal system	monoclinic	monoclinic
Space group	$P2_1/c$	$P2_1/n$
a/Å	19.851(5)	17.797(4)
b/Å	9.799(3)	15.299(2)
c/Å	25.558(6)	19.885(3)
β/°	96.091(2)	107.21(2)
U/Å^3	4943(2)	5172(2)
Z	4	4
F(000)	2220	2280
ρ (calcd)/g cm^{-3}	1.483	1.491
μ (Mokα)/cm^{-1}	4.607	4.890
Diffractometer	CAD4F Enraf-Nonius	IPDS Stoe
Monochromator	graphite	graphite
Radiation	MoKα (λ = 0.71073)	MoKα (λ = 0.71073)
Detector distance/mm		80
Scan mode	ω/2θ	φ
φ range/deg		0 < φ < 200
φ incr./deg		1
Scan range θ/deg	0.8 + 0.345tanθ	
Exposure time/min		3
2θ range/deg	3.0 < 2θ < 40	7.8 < 2θ < 48.2
No. of rflns collected	5095	32249
No. of independent rflns (R_m)	4586 (0.011)	8123 (0.062)
Reflections used, [$I > 2\sigma(I)$]	3060	5571
R	0.0554	0.0605
R_w	0.0645	0.0795
Weighting scheme	Chebyshev	Chebyshev
Coefficient A_r	5.67, 0.553, 4.14	1.79, 0.914, 0.937, −0.348
GOF	1.09	0.92
LS parameters	599	684

Spex Fluorolog FL 111 spectrofluorimeters. Emission quantum yields for the two ligands **4** and **5** were determined in argon-degassed ethanol solutions with respect to the reference 1,3,5-triphenylbenzene (Aldrich, 97%), the quantum yield of which in cyclohexane is 0.27.[11a] 2-2′-Bipyridine (bpy) and 2,2′:6′,2″-terpyridine (tpy) are Aldrich commercial products with purities of 99.5% and 98%, respectively. Emission quantum yields for argon-degassed aqueous solutions of the complexes were determined relative to an aqueous solution of $[Ru(bpy)_3]^{2+}$ (Strem Chemicals, 99%) using $\phi_E = 0.042$ as a reference.[11b] Excitation spectra are corrected from the lamp spectrum by using a program supplied with the instrument. Emission spectra and luminescence excitation spectra have been obtained at room temperature for ligands and complexes and at 77 K for complexes. At 77 K, we used cylindrical cells and the solutions were cooled in a quartz dewar containing liquid nitrogen. For spectroscopic measurements, the optical density of the solutions has been adjusted to 0.1 at the excitation wavelength. The two laser flash photolysis spectrometers used for these investigations have been described in detail elsewhere.[12] In the first one, the excitation source is an excimer laser (Lambda Physik EMG100, 308 nm pulses of 10 ns duration and 150 mJ energy). The second one uses a Nd : YAG laser (Quantel, 353 nm, pulses of 3 ns duration and 100 mJ energy).[12] For the measurements of emission lifetimes, we used solutions with absorption optical densities close to 0.8 at 308 nm.

Cyclic voltammetry

Cyclic voltammetry curves were recorded with a Wenking system (Model 81 potentiostat) using a Pt button (Solea Tacussel EDI 101T) as the working electrode and a platinum wire of 1 mm diameter as the counter-electrode. The working electrode was carefully polished with diamond sprays (Struers) and rinsed with ethanol before each potential run. Acetonitrile (Aldrich, spectrophotometric grade, 99.5%) was used as the solvent and 0.1 mol l^{-1} tetrabutylammonium tetrafluoroborate ($Bu^t_4NBF_4$) (Janssen, 99%) as the supporting electrolyte. These chemicals were used as received. Potentials were measured with respect to the saturated calomel electrode (SCE) and the scan rate was 0.2 V s^{-1}.

Results and Discussion

Ligands

Synthesis of 4 and 5. The synthesis of ligands **4** and **5** is outlined in Scheme 2. The condensation of ketone **1**[13] with the appropriate α,β-unsaturated ketones **2** or **3**, in a 1 : 1 ratio, results in the diene derivatives, which ring-closed *in situ* with ammonium acetate to give the desired ligand with good yields (see *Experimental*). The α,β-unsaturated ketones are prepared by the alkylation of the corresponding enaminones with 3-(2,2-dimethylethoxy)propylmagnesium chloride under the previously described conditions.[14] It is important to point out that the condensation of **1** with **3** in the presence of ammonium acetate in a solvent such as tetramethylurea (TMU) at 90 °C gives a mixture of **5** with the 1,4-addition isomers in a 55 : 1 ratio in 55% yield. However, if this condensation is carried out under the conditions recently described by Bell *et al.*,[15] the yield is only 25% with a 25 : 15 ratio for **5** to the 1,4-addition isomers.

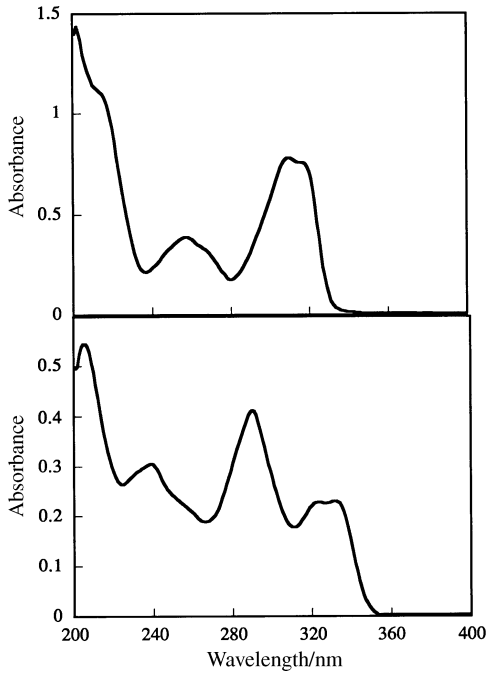

Fig. 1 Absorption spectra of **4** (upper) and **5** (lower) in ethanol (5×10^{-5} mol l^{-1})

Absorption. The electronic absorption spectra of **4** and **5** are shown in Fig. 1. The corresponding absorption maxima, as well as those of bpy and tpy, are presented in Table 2. The bpy molecule may exist in two distinct conformations: *cis* and *trans*.[16] In solution, bpy is preferentially in its *trans* conformation. In ethanol, the *trans* conformer spectrum presents two absorption bands with maxima at 237 and 283 nm. In the *cis* conformer, the absorption maxima are shifted to the red and the band of highest wavenumber is split.[16] In the case of **4**, only the *cis* conformation is possible. Its absorption spectrum [Fig. 1 (upper)] is similar to that of *cis*-bpy with maxima at 259 and 310 nm and a shoulder at 318 nm (Table 2).

The free ligand **5** may be described as a bipyridine with a third pyridine at the 4 position, or as a terpyridine in a locked *cis–trans* conformation. Indeed, tpy presents three conformations: *cis–cis*, *cis–trans* and *trans–trans*. In solution the *trans–trans* conformation is favoured and its absorption spectrum presents maxima at 234 and 280 nm. A third band, at 325 or 320 nm, may be attributed to the existence of small amounts of the *cis–cis* and *cis–trans* conformers, respectively.[16] The absorption spectrum of **5** (Fig. 1) presents four main bands

Table 2 Absorption and emission data for organic ligands in ethanol at room temperature

Ligand	Absorption λ_{max}/nm (ε_{max}/l mol^{-1} cm^{-1})	Emission λ_{max}/nm	ϕ_F	$E_{1/2}$/V *vs.* SCE[a]
bpy	283 (10200), 237 (7700)[b]	—	—	−2.20
tpy	280 (17620), 248sh (14950), 234 (18510)	334	0.003	−2.15[c]
4	318sh (13990), 310 (14990), 259 (7160)	350	0.013	−2.30
5	333 (4800), 324 (4750), 291 (8730), 240 (7130)	367	0.006	−2.05

[a] Redox potentials were measured in acetonitrile *vs.* SCE (saturated calomel electrode) at room temperature with 0.1 mol l^{-1} $[CH_3(CH_2)_3]_4NBF_4$ as the supporting electrolyte and a scanning rate of 200 mV s^{-1}. [b] Ref. 16. [c] Irreversible, ref. 23.

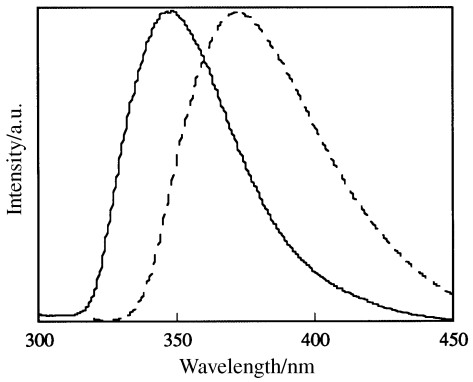

Fig. 2 Fluorescence spectrum of **4** (full line) and **5** (dotted line) in ethanol

with maxima at 333, 324, 291 and 240 nm. It is different from that of 2,2′-bipyridine, but similar to that of the *cis–trans* conformer of tpy. It should be noted that for these *N*-heterocyclic ligands, one can expect an absorption band above 300 nm due to the n–π* transitions. However in ligands **4** and **5**, the related extinction coefficients are too high for such n–π* transitions. Consequently and by analogy with bpy and tpy, we have attributed the absorption bands to $\pi \rightarrow \pi^*$ transitions.

Electrochemistry. Peak potentials of the organic ligands are given in Table 2. The free ligands **4** and **5** showed a reduction wave at −2.30 and −2.05 V *vs.* SCE, respectively. No oxidation wave could be observed out to a potential as positive as +1.5 V *vs.* SCE for either ligand. The reduction potential of **5** is less negative than that of tpy, bpy and **4**. This means that **5** is easier to reduce than the other ligands, contrary to what is expected from its electron-rich structure.

Emission. Ligands **4** and **5** present a fluorescence emission with maxima at 350 and 367 nm, respectively (Table 2, Fig. 2). We have also determined the luminescence excitation spectra of these ligands and they are in good agreement with the corresponding absorption spectra. This result shows that the ligand emissions are not due to an impurity. In Table 2, the corresponding quantum yields ϕ_F (0.013 and 0.006) are also given; **4** is two times more fluorescent than **5**. These emissions are more intense than that of tpy. The existence of a fluorescence emission is *a priori* surprising, as long as simple heterocyclic compounds such as pyridine and bpy are considered to be nonfluorescent or to exhibit a very weak fluorescence.[17] Such a fluorescence has also been observed recently by Thummel and collaborators[4a] for ligands based on benzo[*g*]quinoline, the structure of which is similar to that of **4** and **5**. A possible explanation could be related to the rigidity of the molecule. In fact, it is well known that internal conversion is not favoured in rigid molecular structures.[18] Thus, the conversion to the ground state *via* a radiative deactivation process should be enhanced.

Complexes

Synthesis. Ligands **4** and **5** were further used to prepare the complexes $[Ru(bpy)_2(\mathbf{4})][PF_6]_2$ and $[Ru(bpy)_2(\mathbf{5})][PF_6]_2$. These mixed-ligand complexes $[Ru(bpy)_2(\mathbf{L})]^{2+}$were synthesized in the normal fashion by reacting *cis*-$(bpy)_2RuCl_2$ with ligand **L** in absolute ethanol and precipitating the complex by the addition of ammonium hexafluorophosphate.[19]

X-Ray structure. The molecular structures and atom numbering schemes for $[Ru(bpy)_2(\mathbf{4})]^{2+}$ and $[Ru(bpy)_2(\mathbf{5})]^{2+}$ are shown in Fig. 3. Selected bond lengths and angles can be found in Tables 3 and 4. Of the six Ru—N bond lengths, five are in good agreement with the value of 2.056 Å found for $[Ru(bpy)_3]^{2+}$,[20] but the last one, Ru(1)—N(3), is much longer with values of 2.160(6) Å and 2.165(4) Å for $[Ru(bpy)_2(\mathbf{4})]^{2+}$ and $[Ru(bpy)_2(\mathbf{5})]^{2+}$, respectively. This lengthening may be related to the steric influence of the bulky 2-terbutoxypropyl chain. It is worthwhile to note that this longer Ru—N bond is associated with the largest N(1)—Ru(1)—N(3) angle, 106.8(2)° and 103.5(2)°, respectively. However, the bite angles (78.3°, mean value) are identical within experimental error and compare well with the values (78.7°, mean value) observed in other related Ru complexes such as $[Ru(bpy)_2(C_{14}H_{14})N_2]$.[21]

Absorption. The absorption spectral data for $[Ru(bpy)_2(\mathbf{4})]^{2+}$, $[Ru(bpy)_2(\mathbf{5})]^{2+}$ and $[Ru(bpy)_3]^{2+}$ are summarized in Table 5. The absorption spectra of the heteroleptic complexes (Fig. 4) determined in aqueous solution at room temperature are similar to that of $[Ru(bpy)_3]^{2+}$. Accordingly, they exhibit a broad absorption band in the visible region and two bands in the UV region. The first band appears at about 450 nm and the molar extinction coefficients ε (Table 5) for $[Ru(bpy)_2(\mathbf{4})]^{2+}$ and $[Ru(bpy)_2(\mathbf{5})]^{2+}$ complexes are slightly lower than that of the reference complex $[Ru(bpy)_3]^{2+}$. This hypochromic effect may be attributed to a steric constraint of the ligands **4** and **5**. The most intense UV absorption band is located at 290 nm for the heteroleptic complexes and presents a slight bathochromic shift with respect to the reference complex. The second UV band appears at 238 nm as a shoul-

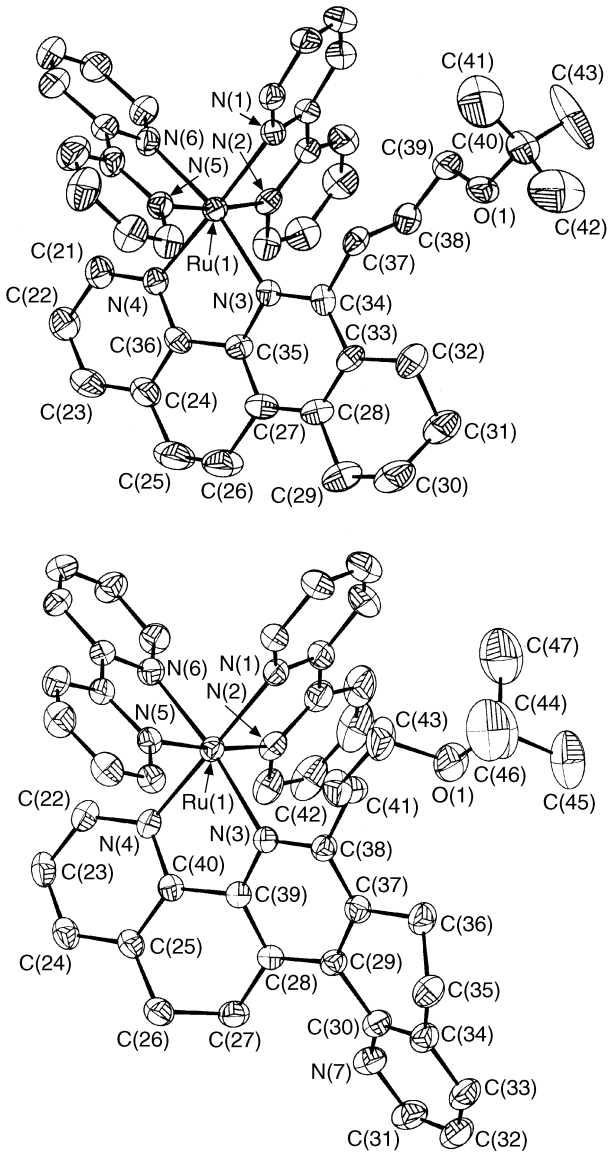

Fig. 3 Molecular view of $[Ru(bpy)_2(\mathbf{4})]^{2+}$ (upper) and $[Ru(bpy)_2(\mathbf{5})]^{2+}$ (lower) with 30% probability thermal ellipsoids depicted

Table 3 Bond lengths (Å). E.s.d.s in parentheses refer to the last significant digit

$[Ru(bpy)_2(\mathbf{4})][PF_6]_2$			
Ru(1)—N(1)	2.075(7)	C(25)—C(26)	1.42(2)
Ru(1)—N(2)	2.074(7)	C(26)—C(27)	1.50(1)
Ru(1)—N(3)	2.160(6)	C(27)—C(28)	1.37(1)
Ru(1)—N(4)	2.058(7)	C(27)—C(35)	1.38(1)
Ru(1)—N(5)	2.069(7)	C(28)—C(29)	1.51(1)
Ru(1)—N(6)	2.048(7)	C(28)—C(33)	1.39(1)
N(3)—C(34)	1.35(1)	C(29)—C(30)	1.55(2)
N(3)—C(35)	1.36(1)	C(30)—C(31)	1.46(2)
N(4)—C(21)	1.34(1)	C(31)—C(32)	1.53(1)
N(4)—C(36)	1.34(1)	C(32)—C(33)	1.52(1)
O(1)—C(39)	1.43(1)	C(33)—C(34)	1.40(1)
O(1)—C(40)	1.44(1)	C(34)—C(37)	1.49(1)
C(5)—C(6)	1.46(1)	C(35)—C(36)	1.45(1)
C(21)—C(22)	1.40(1)	C(37)—C(38)	1.51(1)
C(22)—C(23)	1.35(1)	C(38)—C(39)	1.51(1)
C(23)—C(24)	1.37(1)	C(40)—C(41)	1.45(2)
C(24)—C(25)	1.47(2)	C(40)—C(42)	1.52(2)
C(24)—C(36)	1.38(1)	C(40)—C(43)	1.43(2)
$[Ru(bpy)_2(\mathbf{5})][PF_6]_2$			
Ru(1)—N(1)	2.058(5)	C28)—C(39)	1.401(7)
Ru(1)—N(2)	2.057(5)	C(29)—C(30)	1.496(7)
Ru(1)—N(3)	2.165(4)	C(29)—C(37)	1.393(7)
Ru(1)—N(4)	2.047(5)	C(30)—C(34)	1.412(9)
Ru(1)—N(5)	2.055(4)	C(31)—C(32)	1.37(1)
Ru(1)—N(6)	2.051(4)	C(32)—C(33)	1.37(1)
N(3)—C(38)	1.364(6)	C(33)—C(34)	1.393(9)
N(3)—C(39)	1.347(6)	C(34)—C(35)	1.471(9)
N(4)—C(22)	1.364(7)	C(35)—C(36)	1.52(1)
N(4)—C(40)	1.356(7)	C(36)—C(37)	1.520(8)
N(7)—C(30)	1.332(8)	C(37)—C(38)	1.394(8)
N(7)—C(31)	1.341(8)	C(38)—C(41)	1.499(8)
C(22)—C(23)	1.371(9)	C(39)—C(40)	1.461(7)
C(23)—C(24)	1.362(9)	O(1)—C(43)	1.50(1)
C(24)—C(25)	1.381(8)	O(1)—C(44)	1.37(1)
C(25)—C(26)	1.480(9)	C(41)—C(42)	1.44(1)
C(25)—C(40)	1.393(7)	C(42)—C(43)	1.54(1)
C(26)—C(27)	1.530(9)	C(44)—C(45)	1.517(9)
C(27)—C(28)	1.515(8)	C(44)—C(46)	1.475(8)
C(28)—C(29)	1.390(7)	C(44)—C(47)	1.548(9)

Table 4 Important bond angles (°). E.s.d.s in parentheses refer to the last significant digit

$[Ru(bpy)_2(\mathbf{4})][PF_6]_2$			
N(1)—Ru(1)—N(2)	78.0(3)	C(26)—C(27)—C(35)	119.2(10)
N(1)—Ru(1)—N(3)	106.8(2)	C(28)—C(27)—C(35)	118.3(8)
N(2)—Ru(1)—N(3)	90.9(2)	C(27)—C(28)—C(29)	119.4(10)
N(1)—Ru(1)—N(4)	171.4(3)	C(27)—C(28)—C(33)	120.3(8)
N(2)—Ru(1)—N(4)	95.0(3)	C(29)—C(28)—C(33)	120.3(10)
N(3)—Ru(1)—N(4)	78.2(3)	C(28)—C(29)—C(30)	114.3(11)
N(1)—Ru(1)—N(5)	96.7(3)	C(29)—C(30)—C(31)	110.4(11)
N(2)—Ru(1)—N(5)	173.3(3)	C(30)—C(31)—C(32)	112.5(11)
N(3)—Ru(1)—N(5)	94.7(3)	C(31)—C(32)—C(33)	111.8(10)
N(4)—Ru(1)—N(5)	89.8(3)	C(28)—C(33)—C(32)	122.9(9)
N(1)—Ru(1)—N(6)	82.9(3)	C(28)—C(33)—C(34)	117.8(8)
N(2)—Ru(1)—N(6)	96.2(3)	C(32)—C(33)—C(34)	119.1(9)
N(3)—Ru(1)—N(6)	169.1(3)	N(3)—C(34)—C(33)	123.5(8)
N(4)—Ru(1)—N(6)	92.9(3)	N(3)—C(34)—C(37)	116.9(8)
N(5)—Ru(1)—N(6)	78.8(3)	C(33)—C(34)—C(37)	119.5(8)
Ru(1)—N(3)—C(34)	131.7(6)	N(3)—C(35)—C(27)	123.9(8)
Ru(1)—N(3)—C(35)	112.3(5)	N(3)—C(35)—C(36)	116.5(7)
C(34)—N(3)—C(35)	116.0(7)	C(27)—C(35)—C(36)	119.6(8)
Ru(1)—N(4)—C(21)	124.5(7)	N(4)—C(36)—C(24)	122.4(9)
Ru(1)—N(4)—C(36)	116.4(6)	N(4)—C(36)—C(35)	116.7(7)
C(21)—N(4)—C(36)	119.0(8)	C(24)—C(36)—C(35)	121.0(9)
C(39)—O(1)—C(40)	118.2(8)	C(34)—C(37)—C(38)	114.2(7)
N(4)—C(21)—C(22)	120.3(10)	C(37)—C(38)—C(39)	113.4(8)
C(21)—C(22)—C(23)	120.7(10)	O(1)—C(39)—C(38)	106.7(7)
C(22)—C(23)—C(24)	119.2(10)	O(1)—C(40)—C(41)	108.5(10)
C(23)—C(24)—C(25)	121.1(11)	O(1)—C(40)—C(42)	102.3(10)
C(23)—C(24)—C(36)	118.5(10)	C(41)—C(40)—C(42)	112.8(15)
C(25)—C(24)—C(36)	120.3(10)	O(1)—C(40)—C(43)	113.0(9)
C(24)—C(25)—C(26)	116.7(11)	C(41)—C(40)—C(43)	110.6(16)
C(25)—C(26)—(C27)	118.1(10)	C(42)—C(40)—C(43)	109.4(15)
C(26)—C(27)—C(28)	122.3(10)		
$[Ru(bpy)_2(\mathbf{5})][PF_6]_2$			
N(1)—Ru(1)—N(2)	78.2(2)	C(39)—C(29)—C(37)	118.4(5)
N(1)—Ru(1)—N(3)	103.5(2)	N(7)—C(30)—C(29)	118.6(5)
N(2)—Ru(1)—N(3)	86.9(2)	N(7)—C(30)—C(34)	124.1(5)
N(1)—Ru(1)—N(4)	175.9(2)	C(29)—C(30)—C(30)	117.3(5)
N(2)—Ru(1)—N(4)	97.8(2)	N(7)—C(31)—C(32)	123.3(7)
N(3)—Ru(1)—N(4)	78.4(2)	C(31)—C(32)—C(33)	119.6(6)
N(1)—Ru(1)—N(5)	96.8(2)	C(32)—C(33)—C(34)	119.3(7)
N(2)—Ru(1)—N(5)	173.2(2)	C(30)—C(34)—C(33)	116.6(6)
N(3)—Ru(1)—N(5)	99.3(2)	C(30)—C(34)—C(35)	118.6(5)
N(4)—Ru(1)—N(5)	86.5(2)	C(33)—C(34)—C(35)	124.8(6)
N(1)—Ru(1)—N(6)	83.9(2)	C(34)—C(35)—C(36)	111.0(6)
N(2)—Ru(1)—N(6)	95.5(2)	C(35)—C(36)—C(37)	109.6(5)
N(3)—Ru(1)—N(6)	172.6(2)	C(29)—C(37)—C(36)	119.0(5)
N(4)—Ru(1)—N(6)	94.3(2)	C(29)—C(37)—C(38)	120.2(5)
N(5)—Ru(1)—N(6)	78.8(2)	C(36)—C(37)—C(38)	120.8(5)
Ru(1)—N(3)—C(38)	131.2(3)	N(3)—C(38)—C(37)	121.2(5)
Ru(1)—N(3)—C(39)	111.3(3)	N(3)—C(38)—C(41)	119.4(5)
C(38)—N(3)—C(39)	117.1(4)	C(37)—C(38)—C(41)	119.4(5)
Ru(1)—N(4)—C(22)	127.0(4)	N(3)—C(39)—C(28)	124.5(5)
Ru(1)—N(4)—C(40)	116.1(3)	N(3)—C(39)—C(40)	116.4(4)
C(22)—N(4)—C(40)	116.6(5)	C(28)—C(39)—C(40)	119.1(5)
N(4)—C(22)—C(23)	122.2(5)	N(4)—C(40)—C(25)	123.3(5)
C(22)—C(23)—C(24)	120.5(5)	N(4)—C(40)—C(39)	115.6(4)
C(23)—C(24)—C(25)	119.2(5)	C(25)—C(40)—C(39)	121.0(5)
C(24)—C(25)—C(26)	123.2(5)	C(43)—O(1)—C(44)	116.1(7)
C(24)—C(25)—C(40)	118.1(5)	C(38)—C(41)—C(42)	116.3(7)
C(26)—C(25)—C(40)	118.7(5)	C(41)—C(42)—C(43)	114.6(10)
C(25)—C(26)—C(27)	111.4(5)	O(1)—C(43)—C(42)	104.8(8)
C(26)—C(27)—C(28)	111.4(5)	O(1)—C(44)—C(45)	109.1(8)
C(27)—C(28)—C(29)	124.9(5)	O(1)—C(44)—C(46)	114.0(8)
C(27)—C(28)—C(39)	117.9(5)	C(45)—C(44)—C(46)	111.5(8)
C(29)—C(28)—C(39)	117.2(5)	O(1)—C(44)—C(47)	106.7(8)
C(28)—C(29)—C(30)	123.0(5)	C(45)—C(44)—C(47)	105.5(8)
C(28)—C(29)—C(37)	118.6(5)	C(46)—C(44)—C(47)	109.6(9)

der for $[Ru(bpy)_2(\mathbf{4})]^{2+}$ and at 242 nm for $[Ru(bpy)_2(\mathbf{5})]^{2+}$. Both UV absorption bands present an hypochromic effect with respect to $[Ru(bpy)_3]^{2+}$. By analogy with $[Ru(bpy)_3]^{2+}$, the absorption band at about 450 nm is attributed to a metal-to-ligand charge transfer (MLCT) transition,[3,22] the UV band at about 290 nm is attributed to a $\pi \rightarrow \pi^*$ ligand-centred (LC) transition, whereas the band at 240 nm is attributed to a superposition of LC and LMCT (ligand-to-metal charge transfer) transitions.[21]

Electrochemistry. The redox potentials of $[Ru(bpy)_2(\mathbf{4})]^{2+}$ and $[Ru(bpy)_2(\mathbf{5})]^{2+}$ as determined by cyclic voltammetry are also reported in Table 5. Their voltammograms are comparable to that of the reference complex $[Ru(bpy)_3]^{2+}$. The intensity of the anodic current of the redox couple of each mononuclear complex varies linearly with the square root of the potential scanning rate. This behaviour shows that the heteroleptic complexes exhibit characteristics close to that of the theoretical model. This demonstrates a rapid and reversible monoelectronic charge transfer.[23] A wave is observed at 1.27 V *vs.* SCE in the oxidation mode. This wave corresponds to an oxidation centred on the metal ($Ru^{II} \rightarrow Ru^{III} + e$). In the reduction mode, three reversible waves are observed at −1.30, −1.54 and −1.90 V *vs.* SCE for $[Ru(bpy)_2(\mathbf{4})]^{2+}$ and at −1.30, −1.51 and −1.75 V *vs.* SCE for $[Ru(bpy)_2(\mathbf{5})]^{2+}$. These reductions occur on the orbitals centred on the ligands.[24] Although the free ligand **5** is easier to reduce than bpy, according to their reduction potential (Table 2), the similarities of the first two reduction potentials of both complexes to that of $[Ru(bpy)_3]^{2+}$ indicate that the first reductions take place on the nonsubstituted bpy of the complexes $[Ru(bpy)_2(\mathbf{4})]^{2+}$ and $[Ru(bpy)_2(\mathbf{5})]^{2+}$ according to:

$$[Ru^{II}(bpy)_2(\mathbf{L})]^{2+} + e \rightarrow [Ru^{II}(bpy^{\cdot -})(bpy)(\mathbf{L})]^{+}$$

$$[Ru^{II}(bpy^{\cdot -})(bpy)(\mathbf{L})]^{+} + e \rightarrow [Ru^{II}(bpy^{\cdot -})(bpy^{\cdot -})(\mathbf{L})]$$

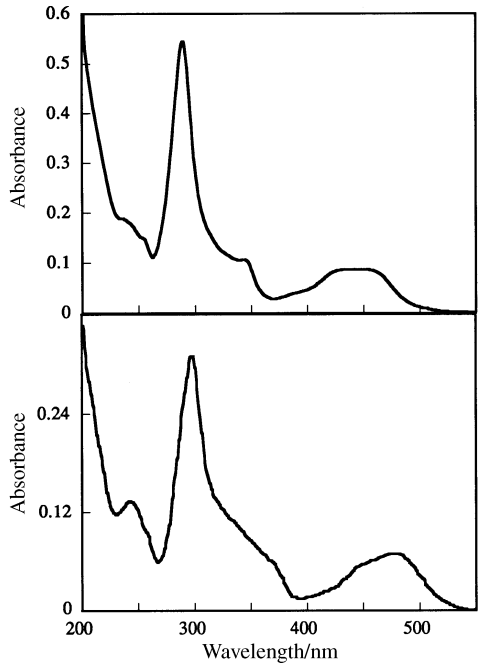

Fig. 4 Absorption spectrum of $[Ru(bpy)_2(\mathbf{4})]^{2+}$ (9×10^{-6} mol l^{-1}) (upper) and $[Ru(bpy)_2(\mathbf{5})]^{2+}$ (8×10^{-6} mol l^{-1}) (lower) in water

Consequently, the third reduction potential for both heteroleptic complexes probably involves ligands **4** and **5** according to:

$$[Ru^{II}(bpy^{\cdot -})(bpy^{\cdot -})(\mathbf{L})] + e \rightarrow [Ru^{II}(bpy^{\cdot -})(bpy^{\cdot -})(\mathbf{L}^{-})]^{-}$$

Emission. The emission data determined at room temperature and at 77 K for $[Ru(bpy)_2(\mathbf{4})]^{2+}$ and $[Ru(bpy)_2(\mathbf{5})]^{2+}$, as well as for $[Ru(bpy)_3]^{2+}$, are collected in Table 6. The emission spectra of $[Ru(bpy)_2(\mathbf{4})]^{2+}$ and $[Ru(bpy)_2(\mathbf{5})]^{2+}$ in aqueous solution (Table 6) are similar to that of the reference complex $[Ru(bpy)_3]^{2+}$ but with a much lower intensity. Both spectra present a large emission band centred at about 614 nm (16290 cm^{-1}). This value corresponds to a bathochromic shift (160 cm^{-1} in water) with respect to $[Ru(bpy)_3]^{2+}$. This shift is similar to that obtained for the absorption spectra. By analogy with the reference complex $[Ru(bpy)_3]^{2+}$, we assign the luminescence of complexes $[Ru(bpy)_2(\mathbf{4})]^{2+}$ and $[Ru(bpy)_2(\mathbf{5})]^{2+}$ to triplet MLCT states.

The emission quantum yields ϕ_E of the heteroleptic complexes $[Ru(bpy)_2(\mathbf{4})]^{2+}$ and $[Ru(bpy)_2(\mathbf{5})]^{2+}$ in aqueous solution at room temperature are 100 and 50 times less intense than that of $[Ru(bpy)_3]^{2+}$, respectively (Table 6). Moreover, and as expected from the emission data, the emission lifetimes of the excited states τ measured by laser flash photolysis are only equal to 10 ns, whereas that of the complex $[Ru(bpy)_3]^{2+}$ is 800 ns (Table 6). We have also observed for the complexes $[Ru(bpy)_2(\mathbf{4})]^{2+}$ and $[Ru(bpy)_2(\mathbf{5})]^{2+}$ a weak contribution from a long emission, which is probably due to an impurity. The decrease of ϕ_E and τ is probably related to a steric hindrance induced by the 2-terbutoxypropyl chain of **4** or **5** substituted in the position adjacent to N(3), which is the closest nitrogen atom of **4** or **5** to the substituent.[25] As shown by crystal studies, this effect is probably responsible for the lengthening of the metal—N(3) bond (Fig. 3). Indeed, the X-ray crystallographic data demonstrate that the Ru—N(3) distance is 2.16 Å whereas the length of the five other Ru—N bonds is 2.05 Å, similar to the 2.056 Å found in $[Ru(bpy)_3]^{2+}$.[26] Consequently, the octahedral geometry of the complexes is distorted. This distortion reduces the ligand field strength and probably lowers the energy of the triplet ^{3}dd excited state, thus allowing a more efficient quenching of the ^{3}MLCT excited state by this ^{3}dd state. In other words, besides the radiative and direct nonradiative processes, the lowest excited MLCT state may be deactivated *via* a thermal population of a higher excited ligand-field state, which undergoes very efficient radiationless decay to the ground state.

We have also undertaken measurements at 77 K for the two complexes $[Ru(bpy)_2(\mathbf{4})]^{2+}$ and $[Ru(bpy)_2(\mathbf{5})]^{2+}$ in ethanol solutions (Fig. 5). Results are quoted in Table 6. As expected, the emission spectra are better resolved than at room temperature. Two maxima are observed at 588 and 634 nm, with a shoulder at 685 nm, for $[Ru(bpy)_2(\mathbf{4})]^{2+}$. Similarly, in the case of $[Ru(bpy)_2(\mathbf{5})]^{2+}$, two emission bands appear at 582 and 630 nm, with a shoulder at 685 nm. These results are similar to that observed for $[Ru(bpy)_3]^{2+}$. It should be

Table 5 Absorption parameters in aqueous solution and electrochemical data in acetonitrile for ruthenium(II) complexes

		$E_{1/2}$/V *vs.* SCE[a]	
Complex	λ_{max}/nm (ε_{max}/l mol^{-1} cm^{-1})	Oxidation	Reduction
$[Ru(bpy)_3]^{2+}$	450 (13800), 286 (98000), 244 (27000)	1.30	−1.29, −1.48, −1.72
$[Ru(bpy)_2(\mathbf{4})]^{2+}$	451 (8750), 290 (53180), 238sh (17870)	1.27	−1.30, −1.54, −1.90
$[Ru(bpy)_2(\mathbf{5})]^{2+}$	453 (12530), 289 (55880), 242 (23820)	1.26	−1.30, −1.51, −1.75

[a] Redox potentials were measured in acetonitrile *vs.* SCE at room temperature with 0.1 M $[CH_3(CH_2)_3]_4NBF_4$ as the supporting electrolyte and a scanning rate of 200 mV s^{-1}.

Table 6 Emission parameters for ruthenium(II) complexes at room temperature and at 77 K

		Room temperature				77 K		
Complex	Solvent	λ_{max}/nm	$\bar{\nu}_{max}$/cm^{-1}	ϕ_E	τ/ns	λ_{max}/nm	E_T/cm^{-1}	τ/μs
$[Ru(bpy)_3]^{2+}$	Water	608	16450	0.042[a]	800			
	Ethanol	601	16640			580, 628, 685sh	15850	5.2[b]
$[Ru(bpy)_2(\mathbf{4})]^{2+}$	Water	615	16260	0.00070	10			
	Ethanol	615	16260			588, 634, 685sh	15730	5.4
$[Ru(bpy)_2(\mathbf{5})]^{2+}$	Water	613	16310	0.00035	9			
	Ethanol	605	16530			582, 630, 685sh	15810	5.5

[a] Ref. 11. [b] Ref. 28.

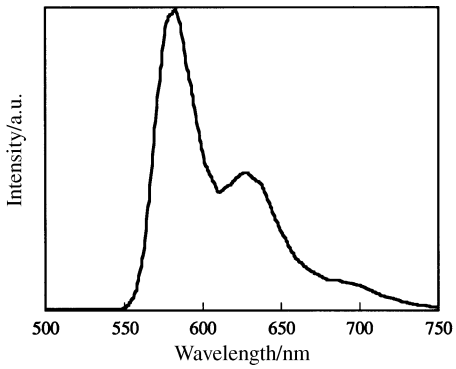

Fig. 5 Luminescence spectrum of $[Ru(bpy)_2(\mathbf{5})]^{2+}$ at 77 K in ethanol

pointed out that these emissions correspond to a constant vibrational progression of 1250 cm^{-1}, similar to that determined for the reference. We also note that the maximum emission is shifted to the red when the temperature is decreased. The shift corresponds to an energy difference of 750 cm^{-1} for $[Ru(bpy)_2(\mathbf{4})]^{2+}$ (from 615 nm at 298 K to 588 nm at 77 K) and 650 cm^{-1} for $[Ru(bpy)_2(\mathbf{5})]^{2+}$ (from 605 nm at 298 K to 582 nm at 77 K). This effect is due to the change from a fluid to a solid medium.[27] In Table 6 are also given the triplet state energies E_T of the complexes. These values have been estimated by considering that the short-wavelength vibrational band of the emission spectra at 77 K corresponds to the 0–0 transition. The triplet state energies of the heteroleptic complexes are similar to that of $[Ru(bpy)_3]^{2+}$.

Concerning the emission lifetime, it may be recalled that the nonradiative deactivation processes are unfavoured at low temperature, thus increasing considerably the lifetime of the excited state at 77 K. For the two heteroleptic complexes, this lifetime is 5.5 μs, a value close to that of the excited state of the reference complex (5.2 μs).[28] All these results show that, as for the reference complex $[Ru(bpy)_3]^{2+}$, the luminescence of $[Ru(bpy)_2(\mathbf{4})]^{2+}$ and $[Ru(bpy)_2(\mathbf{5})]^{2+}$ is clearly due to the triplet ^{3}MLCT state and that the orbital involved in the light-induced charge transfer lies on the bipyridine ligands (and not on **4** or **5**), as was the case for the orbital involved in the first electrochemical reduction step. In other words, the optical and redox orbitals are of a similar nature and the MLCT excited state of the heteroleptic complexes $[Ru(bpy)_2(\mathbf{L})]^{2+}$ corresponds to the Ru → bpy transition.

Conclusion

In this work, we have prepared, characterized and studied the photophysical properties of two new ligands **4** and **5**, which are annelated derivatives of 2,2′-bipyridine. We also report the results concerning two ruthenium(II) heteroleptic complexes $[Ru(bpy)_2(\mathbf{4})]^{2+}$ and $[Ru(bpy)_2(\mathbf{5})]^{2+}$ involving these ligands. Contrary to 2,2-bipyridine, we observed for the free ligands **4** and **5** a fluorescence emission probably due to the rigidity of their molecular structures. The heteroleptic complexes $[Ru(bpy)_2(\mathbf{4})]^{2+}$ and $[Ru(bpy)_2(\mathbf{5})]^{2+}$ present an emission similar to that of the reference complex $[Ru(bpy)_3]^{2+}$. Meanwhile, the emission quantum yield and the emission lifetimes of the excited states are weaker than that of $[Ru(bpy)_3]^{2+}$. We have attributed these effects to the steric hindrance by the 2-terbutoxypropyl chain and not to the rigidity of the ligands. In fact, the adjacent position of the 2-terbutoxypropyl substituent with respect to the nitrogen of **4** or **5** engaged in the coordination, disturbed the octahedral structure with a stretching of the Ru—N(3) bond. This explanation is supported by the reported crystallographic data, which clearly show the lengthening of the Ru—N(3) distance (2.16 Å as compare to 2.05 Å for the other Ru—N bonds). As a consequence, the ligand-field strength is decreased and the probability of nonradiative processes is increased.

Acknowledgements

We thank Mrs A. Barat (Université Paris-Sud) for technical assistance.

References

1 (*a*) E. Amouyal, *Sol. Energy Mater. Sol. Cells*, 1995, **38**, 249. (*b*) E. Amouyal in *Homogeneous Photocatalysis*, ed. M. Chanon, J. Wiley, Chichester, 1997, ch. 8, p. 263.
2 A. Hatzidimitriou, A. Gourdon, J. Devillers, J. P. Launay, E. Mena and E. Amouyal, *Inorg. Chem.*, 1996, **35**, 2212.
3 A. Juris, V. Balzani, F. Barigelletti, S. Campagna, P. Belser and A. Von Zelewsky, *Coord. Chem. Rev.*, 1988, **84**, 85.
4 (*a*) E. Taffarel, S. Chirayil and R. P. Thummel, *J. Org. Chem*, 1994, **59**, 823. (*b*) R. P. Thummel, *Synlett*, 1991, 1. (*c*) P. Caluwe, *Tetrahedron*, 1980, **36**, 2359.
5 (*a*) R. P. Thummel, *Tetrahedron*, 1991, **47**, 6851. (*b*) P. Belser and A. Von Zelewsky, *Helv. Chim. Acta*, 1980, **63**, 1975.
6 (*a*) U. Westerwelle and N. Risch, *Tetrahedron Lett.*, 1993, **34**, 1775. (*b*) R. Keuper and N. Risch, *Liebigs Ann.*, 1996, 717. (*c*) R. Keuper and N. Z. Risch, *Naturforsh.*, 1995, **50B**, 1115.
7 E. Bejan, H. Aït-Haddou, C. Fontenas and G. G. A. Balavoine, unpublished work.
8 A. Altomare, M. C. Burla, M. Camalli, G. Cascarano, C. Giacovazzo, A. Guagliardiand G. Polidori, *J. Appl. Cryst.*, 1994, **27**, 435.
9 E. Prince, *Mathematical Techniques in Crystallography*, Berlin, Springer-Verlag, 1982.
10 (*a*) D. J. Watkin, C. K. Prout, J. R. Carruthers and P. W. Betteridge, *Crystals*, Chemical Crystallography Laboratory, University of Oxford, Oxford, 1996. (*b*) D.J. Watkin, C. K. Prout and L. J. Pearce, *CAMERON*, Chemical Crystallography Laboratory, University of Oxford, Oxford, 1996.
11 (*a*) I. B. Berlman, *Handbook of Fluorescence Spectra of Aromatic Molecules*, Academic Press, New York, 2nd edn., 1971. (*b*) J. Van Houten and R. J. Watts, *J. Am. Chem. Soc.*, 1976, **98**, 4853.
12 E. Amouyal and M. Mouallem-Bahout, *J. Chem. Soc., Dalton Trans.*, 1992, 509.
13 C. Fontenas, H. Aït-Haddou, E. Bejan and G. G. A. Balavoine, unpublished work.
14 E. Bejan, Thesis, Université Paris-Sud, Orsay, France, 1995.
15 T. W. Bell, A. M. Heis, R. T. Ludwig and C. Xiang, *Synlett*, 1996, 79.
16 K. Nakamato, *J. Phys. Chem.*, 1960, **64**, 1420.
17 (*a*) A. Harriman, *J. Photochem.*, 1978, **8**, 205. (*b*) M. S. Henry and M. Z. Hoffman, *J. Phys. Chem.*, 1979, **83**, 61. (*c*) J. Kotlika and Z. R. Grabowsky, *J. Photochem.*, 1979, **11**, 413. (*d*) E. Castelluci and I. Baraldi, *J. Phys. Chem.*, 1990, **94**, 1740.
18 N. J. Turro, *Modern Molecular Photochemistry*, Benjamin/Cummings, Menlo Park, USA, 1978.
19 R. P. Thummel and F. Lefoulon, *Inorg Chem.*, 1987, **26**, 675.
20 D. P. Rillema and D. S. Jones, *J. Chem. Soc., Chem. Commun.*, 1979, 849.
21 R. P. Thummel, F. Lefoulon and J. D. Korp, *Inorg. Chem.*, 1987, **26**, 2370.
22 G. Calzaferri and R. Rytz, *J. Phys. Chem.*, 1995, **99**, 12141.
23 N. E. Tokel-Takvoryan, R. E. Hemigway and A. J. Bard *J. Am. Chem. Soc.*, 1973, **95**, 6582.
24 (*a*) Y. Kawanishi, N. Kitamura, Y. Kim and S. Tazuke, *Sci. Pap. Inst. Phys. Chem. Res.* (*Jpn*), 1984, **78**, 212. (*b*) A. Vlcek, *Chemtracts- Inorg. Chem.*, 1991, **5**, 2144.
25 E. Fujita, S. J. Milder and B. S. Brunschwig, *Inorg. Chem.*, 1992, **31**, 2079.
26 D. P. Rillema, D. S. Jones and H. A. Levy, *J. Chem. Soc., Chem. Commun.*, 1979, 849.
27 F. Barigelletti, A. Juris, V. Belser and A. Von Zelewski, *J. Phys. Chem.*, 1987, **91**, 1095.
28 E. Amouyal, M. Mouallem-Bahout and G. Calzaferri, *J. Phys. Chem.*, 1991, **95**, 7641.

Received in Orsay, France, 11*th July* 1997;
Paper 7/08740C